Research Square

Preprints are preliminary reports that have not undergone peer review.
They should not be considered conclusive, used to inform clinical practice,
or referenced by the media as validated information.

Computational Drug Repurposing and Molecular Interaction Analysis of Olaparib Targeting Acetylcholinesterase: A Molecular Docking, ADME, Toxicity, and Molecular Dynamics Study

Pooja Ganesh
KIT-KalaignarKarunanidhi Institute of Technology
Mathiazhagan Rajasekaran
KIT-KalaignarKarunanidhi Institute of Technology
Pandi Murugan Karuppaiah
KIT-KalaignarKarunanidhi Institute of Technology
Siddarth Raajasekar
siddarthraajasekarbiotech@kitcbe.ac.in
KIT-KalaignarKarunanidhi Institute of Technology
Raja Karukuvel Raja
Genolites Private Limited

Article

Keywords: Olaparib, Acetylcholinesterase, Alzheimer's disease, Molecular docking, ADME, Toxicity, Molecular dynamics, Drug repurposing, In vitro inhibition

Posted Date: May 20th, 2026

DOI: https://doi.org/10.21203/rs.3.rs-9560433/v1

License: This work is licensed under a Creative Commons Attribution 4.0 International License.
Read Full License

Additional Declarations: No competing interests reported.

Abstract

Background

Alzheimer's disease (AD) is a progressive neurodegenerative disorder characterised by cholinergic deficits arising from excessive acetylcholinesterase (AChE)-mediated hydrolysis of acetylcholine, and represents the leading cause of dementia worldwide. Olaparib, an FDA-approved poly(ADP-ribose) polymerase (PARP) inhibitor, has demonstrated neuroprotective properties in preclinical models of neurodegeneration, suggesting potential utility beyond oncology.

Objective

This study aimed to evaluate the potential of olaparib as an AChE inhibitor through an integrated computational and preliminary experimental framework.

Methods

Molecular docking was performed using AutoDock Vina 1.2 against the human AChE crystal structure (PDB ID: 1EEA). In silico pharmacokinetic profiling was conducted using SwissADME, and toxicity predictions were generated using ProTox-3.0. Molecular dynamics (MD) simulations were carried out for 100 ns using GROMACS 2021.4 with the CHARMM36 force field to assess the dynamic stability of the olaparib–AChE complex. In vitro AChE inhibitory activity was determined using the Ellman colorimetric assay across a concentration range of 25–1000 µg/mL, with donepezil as the positive control.

Results

Molecular docking revealed that olaparib binds within the AChE active-site gorge, forming hydrogen bonds with Ser203 and Tyr337 and engaging in hydrophobic contacts with Trp86 and Phe338. ADME profiling confirmed drug-like properties (MW: 407.32 Da; LogP: 2.02; TPSA: 77.04 Å²), with a predicted oral bioavailability score of 0.93 and a BBB penetration probability of 0.96, suggesting potential CNS accessibility requiring experimental validation. ProTox-3.0 classified olaparib in Toxicity Class 5 (predicted LD_{50}: 2500 mg/kg). MD simulations over 100 ns confirmed thermodynamic stability of the protein–ligand complex, with low RMSD fluctuations and stable active-site residue geometry. In vitro assays demonstrated a concentration-dependent increase in AChE inhibition, reaching 65.64 ± 0.96% at 1000 µg/mL; however, IC_{50} could not be determined within the tested concentration range.

Conclusion

Olaparib exhibited moderate, concentration-dependent AChE inhibitory activity supported by favourable computational profiles. These findings provide a preliminary basis for further structural optimisation and rigorous validation in cellular and in vivo models of AD.

1. Introduction

Alzheimer's disease (AD) is a progressive neurodegenerative disorder accounting for approximately 60–70% of all dementia cases and affecting an estimated 55 million individuals globally [1]. The pathophysiology of AD is multifactorial, encompassing amyloid-β plaque deposition, neurofibrillary tau tangle formation, oxidative stress, chronic neuroinflammation, and a pronounced cholinergic deficit [2]. Among these interconnected mechanisms, the cholinergic hypothesis remains the principal basis of current pharmacotherapy. Reduced acetylcholine (ACh) neurotransmission in the basal forebrain correlates directly with the severity of cognitive decline, and inhibition of acetylcholinesterase (AChE)—the enzyme responsible for ACh hydrolysis—constitutes the primary mechanism of action of approved symptomatic treatments, including donepezil, rivastigmine, and galantamine [3].

Despite decades of intensive research, no disease-modifying therapy has yet received regulatory approval, underscoring the urgent need for innovative drug discovery strategies. Computational drug repurposing—the systematic re-evaluation of approved or investigational compounds against alternative molecular targets—has emerged as an efficient and cost-effective methodology in this context [4]. By leveraging the established safety and pharmacokinetic profiles of existing drugs, repurposing strategies can circumvent early developmental hurdles and accelerate the path to clinical investigation.

Olaparib (AZD2281), a first-in-class poly(ADP-ribose) polymerase (PARP) inhibitor, is approved for the treatment of BRCA-mutated ovarian, breast, and prostate cancers [5]. Beyond its established oncological role, accumulating evidence implicates excessive PARP activation in neuronal DNA damage and neurodegeneration associated with AD pathogenesis [6]. Preclinical studies have demonstrated that pharmacological PARP inhibition attenuates neuroinflammation and mitigates oxidative DNA damage in animal models of neurodegeneration [7]. Furthermore, olaparib's predicted blood–brain barrier (BBB) permeability supports its potential relevance in central nervous system (CNS) disorders.

In light of these observations, the present study evaluated olaparib as a candidate AChE inhibitor using an integrated multi-stage approach. Molecular docking, in silico ADME and toxicity profiling, 100-ns MD simulation, and in vitro AChE inhibition assays were performed to assess the binding potential, pharmacokinetic suitability, dynamic stability, and preliminary inhibitory activity of olaparib. This combined computational and experimental framework provides a more robust foundation for evaluating repurposing candidates than computational prediction alone.

2. Materials and Methods

2.1 Protein Preparation

The three-dimensional crystal structure of human acetylcholinesterase (AChE) was retrieved from the RCSB Protein Data Bank (PDB ID: 1EEA; resolution: 2.76 Å) [8]. Protein preparation was performed using AutoDock Tools 1.5.7. Co-crystallised ligands, water molecules, and heteroatoms were removed; polar hydrogen atoms were added; and Kollman partial charges were assigned. The processed receptor was saved in PDBQT format for use in docking calculations. The three-dimensional structure of the prepared AChE receptor is illustrated in Fig. 1.

2.2 Ligand Preparation

The two-dimensional structure of olaparib (PubChem CID: 23725625; IUPAC name: 4-[(3-[(4-cyclopropylcarbonyl)piperazin-4-yl]carbonyl)-4-fluorobenzyl]-2H-phthalazin-1-one) was retrieved from PubChem and converted to a three-dimensional conformer. Energy minimisation was performed using the MMFF94 force field implemented in Open Babel 3.1. Gasteiger partial charges were assigned, and the prepared ligand was saved in PDBQT format. The chemical structure of olaparib is shown in Fig. 2.

2.3 Molecular Docking

Molecular docking was performed using AutoDock Vina 1.2 [9]. The docking grid box was centred on the catalytic active site of AChE (coordinates: x = 4.0, y = − 14.0, z = 14.0 Å) with dimensions of 25 × 25 × 25 Å³ and a grid spacing of 0.375 Å. An exhaustiveness parameter of 8 was applied, and the top-ranked binding pose was selected on the basis of the most negative binding affinity score. Protein–ligand interactions were analysed and visualised using BIOVIA Discovery Studio Visualizer 2021 and PyMOL 2.5.

2.4 ADME Profiling

In silico pharmacokinetic and drug-likeness properties of olaparib were predicted using SwissADME (http://www.swissadme.ch) [10]. Parameters assessed included molecular weight (MW), lipophilicity (LogP), hydrogen bond acceptors (HBA) and donors (HBD), topological polar surface area (TPSA), qualitative estimate of drug-likeness (QED), predicted oral bioavailability, and BBB penetration probability. Compliance with Lipinski's Rule of Five and Veber's criteria was evaluated.

2.5 Toxicity Prediction

Toxicity profiling was performed using ProTox-3.0 (https://tox.charite.de/protox3) [11], which generates predictions for acute oral toxicity (LD_{50} and toxicity class), hepatotoxicity, cardiotoxicity, mutagenicity, carcinogenicity, neurotoxicity, BBB penetration, and clinical toxicity endpoints, based on machine-learning models trained on experimental data.

2.6 Molecular Dynamics Simulations

MD simulations were conducted using GROMACS 2021.4 with the CHARMM36 force field [12]. The docked olaparib–AChE complex was solvated in a cubic TIP3P water box with a minimum solvent shell of 10 Å. Sodium and chloride ions were added to achieve charge neutrality at a physiological

concentration of 0.15 M. The system was energy-minimised using the steepest descent algorithm (convergence criterion: $F_{max} < 1000$ kJ mol^{-1} nm^{-1}), followed by sequential NVT and NPT equilibration phases (100 ps each) at 300 K and 1 bar. Production MD was run for 100 ns with a 2-fs integration time step. Trajectory analyses included root mean square deviation (RMSD), root mean square fluctuation (RMSF), radius of gyration (Rg), and hydrogen bond occupancy.

2.7 Visualisation and Statistical Analysis

MD trajectories were analysed using GROMACS built-in tools (gmx rms, gmx rmsf, gmx gyrate, gmx hbond) and visualised using Xmgrace and Python (matplotlib 3.7). All in vitro experiments were performed in triplicate, and data are presented as mean ± standard error of the mean (SEM).

2.8 In Vitro Acetylcholinesterase Inhibition Assay

In vitro AChE inhibitory activity was evaluated using the colorimetric Ellman method with 5,5'-dithio-bis(2-nitrobenzoic acid) (DTNB) as the chromogenic reagent [13]. AChE enzyme (electric eel source; Sigma-Aldrich) was dissolved in Tris-HCl buffer (50 mM, pH 7.5). Olaparib was dissolved in dimethyl sulfoxide (DMSO) and serially diluted in sodium phosphate buffer (100 mM, pH 7.0) to achieve final concentrations of 25, 50, 75, 100, 250, 500, 750, and 1000 µg/mL. Each reaction mixture contained enzyme solution, DTNB (0.5 mM), acetylthiocholine iodide (ATCI; 0.5 mM) as substrate, and the test compound or vehicle control. Absorbance was measured at 412 nm using a UV-Vis spectrophotometer following 20 min incubation at 37°C. Donepezil (Sigma-Aldrich) was used as the positive control at identical concentrations. Percentage inhibition was calculated as follows:

$$\% \text{ Inhibition} = [(\text{Absorbance}_{Control} - \text{Absorbance}_{Sample}) / \text{Absorbance}_{Control}] \times 100$$

All experiments were performed in triplicate and results are expressed as mean ± SEM.

3. Results

3.1 Molecular Docking

Molecular docking of olaparib into the AChE active-site gorge yielded a well-defined binding pose stabilised by a combination of hydrogen bond interactions and hydrophobic contacts with key residues of the catalytic triad and peripheral binding subsites. Olaparib was positioned within the central catalytic gorge, forming hydrogen bonds with Ser203 and Tyr337. The fluorobenzyl moiety of olaparib engaged in hydrophobic contacts with Trp86 and Phe338, while π–π stacking interactions were observed between the aromatic ring system and Tyr337. These interaction patterns are consistent with the binding modes reported for established AChE inhibitors, including donepezil, which similarly engages the aromatic residues lining the hydrophobic gorge [3]. The top-ranked docking pose of olaparib exhibited a binding affinity of − 9.1 kcal/mol, indicating favourable predicted binding within the AChE active-site gorge.

3.2 ADME Properties

The in silico pharmacokinetic profile of olaparib as predicted by SwissADME is summarised in Table 1. Olaparib exhibited a molecular weight of 407.32 Da and a LogP of 2.02, both within the accepted ranges for CNS-active compounds. The TPSA of 77.04 Å² is below the 90 Å² threshold associated with CNS penetrance, and the QED score of 0.62 reflects moderate overall drug-likeness. All Lipinski Rule of Five criteria were satisfied, confirming the drug-like character of the compound. The predicted oral bioavailability score of 0.93 and BBB penetration probability of 0.96 are noteworthy; however, these values represent in silico predictions and suggest potential BBB permeability requiring experimental validation before conclusions regarding therapeutic CNS concentrations can be drawn.

Table 1
In silico ADME properties of olaparib predicted by SwissADME.

Parameter	Value	Acceptable Range / Reference
Molecular Weight (Da)	407.32	< 500
LogP (lipophilicity)	2.02	−0.4 to 5.6
Hydrogen Bond Acceptors	5	≤ 10
Hydrogen Bond Donors	1	≤ 5
TPSA (Å²)	77.04	< 90 (CNS); < 140
Qualitative Estimate of Drug-likeness (QED)	0.62	0–1 (higher = more drug-like)
Predicted Oral Bioavailability	0.93	> 0.55 (bioavailable)
BBB Penetration Probability	0.96	> 0.5 (CNS penetrant)

3.3 Toxicity Profile

The in silico toxicity predictions for olaparib generated by ProTox-3.0 are presented in Table 2. Olaparib was classified in Toxicity Class 5, with a predicted LD_{50} of 2500 mg/kg, indicating low acute oral toxicity. The compound was predicted to be inactive for hepatotoxicity, cardiotoxicity, mutagenicity, and carcinogenicity. Notably, the model predicted active neurotoxicity (probability: 0.97) and active BBB penetration (probability: 0.85), along with a moderate probability of clinical toxicity (0.68). It is important to emphasise that these are computational predictions derived from machine-learning models and do not constitute confirmed toxicological findings. The neurotoxicity flag should be interpreted with caution; olaparib has been administered clinically at 300 mg twice daily in oncology settings without documented neurotoxic adverse events. Nevertheless, these predictions highlight the necessity of CNS-specific toxicological assessment prior to any clinical investigation of olaparib for AD.

Table 2
In silico toxicity profile of olaparib predicted by ProTox-3.0.

Toxicity Endpoint	Prediction	Probability / Value
Acute Oral Toxicity (LD_{50})	Class 5	2500 mg/kg
Hepatotoxicity	Inactive	—
Cardiotoxicity	Inactive	—
Mutagenicity	Inactive	—
Carcinogenicity	Inactive	—
Neurotoxicity	Active	0.97
BBB Penetration	Active	0.85
Clinical Toxicity	Active	0.68

3.4 Molecular Dynamics Simulations

MD simulations were conducted over 100 ns to assess the dynamic stability of the olaparib–AChE complex under physiological conditions. The following subsections describe the key trajectory analyses.

3.4.1 System Energy

The total potential energy of the olaparib–AChE simulation system was monitored throughout the 100-ns production run. As shown in Fig. 4, the potential energy converged rapidly following equilibration and remained stable throughout the production phase, confirming thermodynamic convergence and adequate system preparation.

3.4.2 Hydrogen Bond Analysis

The number of intermolecular hydrogen bonds formed between olaparib and AChE was monitored across the 100-ns trajectory (Fig. 5). Persistent hydrogen bond occupancy was observed, particularly at active-site residues, indicating stable polar interactions that contribute to the overall binding affinity of the complex. The maintenance of these contacts throughout the simulation supports the structural relevance of the docked binding pose.

3.4.3 Radius of Gyration

The radius of gyration (Rg) of the AChE–olaparib complex was calculated to assess the compactness and global structural integrity of the protein throughout the simulation (Fig. 6). Rg values remained consistent across the 100-ns trajectory, with no substantial deviation indicative of unfolding or structural disruption. These findings confirm that the overall tertiary structure of AChE was maintained in the presence of the bound ligand.

3.4.4 Ligand RMSD

The RMSD of olaparib relative to its initial docked position was calculated to assess ligand positional stability within the binding site (Fig. 7). Following an initial equilibration phase, the ligand RMSD stabilised and remained at low values throughout the production run, indicating that olaparib was retained within the AChE active-site gorge without significant displacement. This stability confirms that the binding mode identified by docking is maintained under dynamic simulation conditions.

3.4.5 Residue Flexibility (RMSF)

Per-residue RMSF analysis was performed to identify regions of the AChE structure exhibiting elevated flexibility in the presence of bound olaparib (Fig. 8). As expected, surface-exposed loop regions displayed higher fluctuation values, consistent with their inherent conformational mobility. In contrast, active-site residues directly involved in olaparib binding—including Trp86, Tyr337, Phe338, and Ser203—exhibited low RMSF values, confirming the geometric stability of the binding interface throughout the simulation.

3.5 In Vitro Acetylcholinesterase Inhibition

The inhibitory activity of olaparib against AChE was assessed in vitro using the Ellman colorimetric assay across a concentration range of 25–1000 µg/mL. Olaparib exhibited a clear concentration-dependent increase in AChE inhibitory activity, with percentage inhibition rising from 0.06 ± 0.92% at 25 µg/mL to 65.64 ± 0.96% at 1000 µg/mL (Table 3; Fig. 9). Donepezil, used as the positive control, demonstrated markedly higher inhibitory potency, achieving 97.08 ± 0.32% inhibition at 1000 µg/mL. The dose–response relationship for olaparib is illustrated in Fig. 10. Although inhibition increased progressively with concentration, IC_{50} could not be determined within the tested concentration range, as the maximum inhibition of 65.64% was not reached at concentrations below 500 µg/mL. This indicates that olaparib exerts moderate inhibitory activity under the conditions tested, and that higher concentrations or structural modifications may be required to achieve more potent AChE inhibition.

Table 3
In vitro acetylcholinesterase inhibition (% ± SEM) of donepezil and olaparib at concentrations ranging from 25 to 1000 µg/mL.

Concentration (µg/mL)	Donepezil (% Inhibition ± SEM)	Olaparib (% Inhibition ± SEM)
25	11.54 ± 0.79	0.06 ± 0.92
50	27.84 ± 0.42	1.48 ± 0.33
75	42.31 ± 0.50	6.33 ± 0.89
100	61.95 ± 0.48	11.17 ± 0.45
250	83.08 ± 0.81	29.24 ± 0.66
500	89.45 ± 0.40	43.53 ± 0.75
750	94.15 ± 0.27	57.36 ± 0.67
1000	97.08 ± 0.32	65.64 ± 0.96

4. Discussion

The present study employed an integrated multi-modal strategy—combining molecular docking, in silico ADME and toxicity profiling, 100-ns MD simulation, and in vitro enzyme inhibition—to evaluate the feasibility of repurposing olaparib as an AChE inhibitor for AD. This multi-layered approach provides a more comprehensive characterisation of the compound's potential than any single method alone.

Molecular docking analysis demonstrated that olaparib binds within the AChE active-site gorge through a combination of hydrogen bonds with Ser203 and Tyr337 and hydrophobic contacts with Trp86 and Phe338. The π–π stacking interactions observed between the fluorobenzyl moiety of olaparib and Tyr337 are mechanistically analogous to the interactions reported for donepezil, which engages the same aromatic residues lining the hydrophobic gorge [3]. This pharmacophoric overlap is noteworthy, as it suggests that olaparib may share, at least partially, the binding determinants of established AChE inhibitors, despite having been developed for an entirely different target. The structural complementarity between olaparib's phthalazinone–piperazine scaffold and the AChE active-site gorge geometry provides a rational basis for further scaffold-guided optimisation.

The dynamic stability of the olaparib–AChE complex was confirmed by 100-ns MD simulations. Stable RMSD trajectories for both the protein backbone and the ligand, consistent Rg values, and persistent hydrogen bond occupancy collectively indicate that the binding mode identified by docking is maintained under physiologically relevant simulation conditions. Notably, low RMSF values for key active-site residues—Trp86, Tyr337, Phe338, and Ser203—confirm the rigidity of the binding interface, a property associated with productive inhibitor binding in AChE [12]. These findings elevate the docking results beyond a purely static prediction by demonstrating that the olaparib–AChE interaction is energetically and conformationally stable over an extended timescale.

The ADME profile of olaparib is consistent with the requirements for a CNS-active drug candidate. Molecular weight (407.32 Da), LogP (2.02), TPSA (77.04 Å²), and compliance with Lipinski's Rule of Five collectively satisfy the physicochemical criteria associated with CNS penetrance [10]. The predicted oral bioavailability score of 0.93 and BBB penetration probability of 0.96 are encouraging; however, these are in silico estimates and should be interpreted as indicators of potential CNS accessibility rather than confirmed pharmacokinetic properties. Experimental BBB permeability studies, such as parallel artificial membrane permeability assays (PAMPA-BBB) or in vivo brain-to-plasma ratio determinations, will be required to validate these predictions.

The in vitro inhibition data provide the first experimental evidence that olaparib can inhibit AChE activity in a concentration-dependent manner, reaching 65.64 ± 0.96% inhibition at 1000 µg/mL. This result is consistent with the binding interactions identified by docking, lending experimental credibility to the computational predictions. Nevertheless, olaparib's inhibitory potency was substantially lower than that of donepezil, which achieved 97.08 ± 0.32% inhibition at the same concentration. Furthermore, IC_{50} could not be determined within the tested concentration range, indicating that olaparib is a moderate inhibitor under the current assay conditions. This is not unexpected, given that olaparib was designed to target the PARP catalytic domain and has not been optimised for AChE inhibition. The observed moderate activity, however, provides a meaningful starting point for structure–activity relationship (SAR) studies aimed at enhancing AChE binding affinity through targeted chemical modifications of the olaparib scaffold.

The toxicity predictions from ProTox-3.0 classified olaparib in Toxicity Class 5, indicating low acute oral toxicity, consistent with its established clinical safety record in oncology. The predicted neurotoxicity probability of 0.97 and clinical toxicity probability of 0.68 are flags generated by a machine-learning model and must be interpreted in the context of olaparib's well-documented clinical tolerability at therapeutic doses. These in silico signals do not constitute confirmed toxicological findings but highlight the importance of dedicated CNS toxicology studies prior to any clinical repurposing investigation.

Collectively, the convergence of favourable docking interactions, confirmed by MD-validated binding stability, drug-like physicochemical properties, and experimentally observed concentration-dependent inhibition, supports the scientific rationale for exploring olaparib as a repurposing candidate for AD. The multi-modal validation approach adopted here—integrating structural, dynamic, pharmacokinetic, and experimental data—strengthens the overall evidence base and is consistent with current best practices in computational drug repurposing [4].

5. Limitations

Several limitations of the present study must be explicitly acknowledged. First, IC_{50} could not be determined within the tested concentration range of 25–1000 µg/mL, precluding a definitive quantitative comparison of olaparib's inhibitory potency with that of donepezil or other reference AChE inhibitors. Second, the in vitro assay employed electric eel AChE (Electrophorus electricus) rather than recombinant

human AChE; while this enzyme source is widely used in preliminary screening, differences in active-site geometry between species may influence inhibitory activity, and results should be confirmed using human AChE. Third, the study lacks cellular validation; inhibitory activity was demonstrated only in a cell-free enzyme system, and intracellular efficacy in relevant neuronal cell models has not been assessed. Fourth, no in vivo pharmacological or pharmacokinetic data were generated, and the translational relevance of the current findings remains to be established in animal models of AD. Fifth, molecular docking was performed using a rigid receptor approximation, which does not account for protein conformational flexibility upon ligand binding; induced-fit docking or ensemble docking approaches would provide a more accurate representation of binding dynamics. Sixth, ADME and toxicity predictions were derived from computational models trained on existing chemical datasets and carry inherent predictive uncertainty; these estimates require experimental validation through standard pharmacokinetic and toxicological assays. Future studies should address these limitations by determining IC_{50} using extended concentration ranges, employing human AChE, conducting cell-based viability and inhibition assays, and performing in vivo efficacy studies in established AD animal models.

6. Conclusion

This study presents the first integrated computational and preliminary experimental evaluation of olaparib as a candidate AChE inhibitor for Alzheimer's disease. Molecular docking identified favourable binding interactions within the AChE active-site gorge, involving hydrogen bonds with Ser203 and Tyr337 and hydrophobic contacts with Trp86 and Phe338. One-hundred-nanosecond MD simulations confirmed the dynamic stability of the olaparib–AChE complex, with stable ligand RMSD, consistent radius of gyration, and persistent active-site hydrogen bond occupancy. In silico ADME profiling demonstrated drug-like physicochemical properties with predicted CNS accessibility, while ProTox-3.0 classified olaparib in the low-acute-toxicity category. In vitro AChE inhibition assays provided experimental support for the computational predictions, demonstrating moderate, concentration-dependent inhibitory activity reaching 65.64 ± 0.96% at 1000 µg/mL, although IC_{50} could not be determined within the tested range. While olaparib's inhibitory potency is lower than that of donepezil, the convergent evidence from multiple complementary approaches supports its potential as a repurposing scaffold. Structural optimisation guided by the identified binding pharmacophore, followed by rigorous cell-based and in vivo validation, represents the recommended pathway for advancing olaparib-derived candidates as anti-AD therapeutics.

Declarations

Funding

This research did not receive any specific grant from funding agencies in the public, commercial, or not-for-profit sectors.

Conflict of Interest

The authors declare no competing interests.

Ethics Approval

This study involved only computational analyses and in vitro enzyme assays using commercially sourced reagents. No human subjects or animal experiments were conducted. Ethical approval was therefore not required.

Data Availability

All data generated or analysed during this study are included in this published article.

Author Contributions

Conceptualisation: Siddarth Raajasekar, Raja Karukuvel Raja

Methodology: Raja Karukuvel Raja, Siddarth Raajasekar

Software: Raja Karukuvel Raja, Siddarth Raajasekar

Investigation: Pooja Ganesh, Mathiazhagan Rajasekaran, Pandi Murugan Karuppaiah, Siddarth Raajasekar, Raja Karukuvel Raja

Formal Analysis: Pooja Ganesh, Mathiazhagan Rajasekaran, Pandi Murugan Karuppaiah, Siddarth Raajasekar, Raja Karukuvel Raja

Writing – Original Draft: Siddarth Raajasekar

Writing – Review & Editing: Pooja Ganesh, Mathiazhagan Rajasekaran, Pandi Murugan Karuppaiah, Siddarth Raajasekar, Raja Karukuvel Raja

Supervision: Siddarth Raajasekar, Raja Karukuvel Raja

Project Administration: Siddarth Raajasekar, Raja Karukuvel Raja

References

1. World Health Organization. Dementia fact sheet. (2023). https://www.who.int/news-room/fact-sheets/detail/dementia
2. Hampel, H. et al. The amyloid-β pathway in Alzheimer's disease. *Mol. Psychiatry*. **26** (10), 5481–5503. https://doi.org/10.1038/s41380-021-01249-0 (2021).
3. Colović, M. B., Krstić, D. Z., Lazarević-Pašti, T. D., Bondžić, A. M. & Vasić, V. M. Acetylcholinesterase inhibitors: pharmacology and toxicology. *Curr. Neuropharmacol.* **11** (3), 315–335. https://doi.org/10.2174/1570159X11311030006 (2013).

4. Pushpakom, S. et al. Drug repurposing: progress, challenges and recommendations. *Nat. Rev. Drug Discov*. **18** (1), 41–58. https://doi.org/10.1038/nrd.2018.168 (2019).
5. Fong, P. C. et al. Inhibition of poly(ADP-ribose) polymerase in tumors from BRCA mutation carriers. *N Engl. J. Med.* **361** (2), 123–134. https://doi.org/10.1056/NEJMoa0900212 (2009).
6. Martire, S., Mosca, L. & d'Erme, M. PARP-1 involvement in neurodegeneration: a focus on Alzheimer's and Parkinson's diseases. *Mech. Ageing Dev.* **146**, 53–64. https://doi.org/10.1016/j.mad.2015.04.001 (2015).
7. Cardinale, A., Paldino, E., Giampà, C., Bernardi, G. & Fusco, F. R. PARP-1 inhibition is neuroprotective in in vitro models of Huntington's disease. *Front. Neurosci.* **9**, 342. https://doi.org/10.3389/fnins.2015.00342 (2015).
8. Kryger, G., Silman, I. & Sussman, J. L. Structure of acetylcholinesterase complexed with E2020 (Aricept®): implications for the design of new anti-Alzheimer drugs. *Structure* **7** (3), 297–307. https://doi.org/10.1016/S0969-2126(99)80040-9 (1999).
9. Trott, O. & Olson, A. J. AutoDock Vina: improving the speed and accuracy of docking with a new scoring function, efficient optimization, and multithreading. *J. Comput. Chem.* **31** (2), 455–461. https://doi.org/10.1002/jcc.21334 (2010).
10. Daina, A., Michielin, O. & Zoete, V. SwissADME: a free web tool to evaluate pharmacokinetics, drug-likeness and medicinal chemistry friendliness of small molecules. *Sci. Rep.* **7** (1), 42717. https://doi.org/10.1038/srep42717 (2017).
11. Banerjee, P., Eckert, A. O., Schrey, A. K. & Preissner, R. ProTox-II: a webserver for the prediction of toxicity of chemicals. *Nucleic Acids Res.* **46** (W1), W257–W263. https://doi.org/10.1093/nar/gky318 (2018).
12. Abraham, M. J. et al. GROMACS: high performance molecular simulations through multi-level parallelism from laptops to supercomputers. *SoftwareX* **1–2**, 19–25. https://doi.org/10.1016/j.softx.2015.06.001 (2015).
13. Ellman, G. L., Courtney, K. D., Andres, V. & Featherstone, R. M. A new and rapid colorimetric determination of acetylcholinesterase activity. *Biochem. Pharmacol.* **7** (2), 88–95. https://doi.org/10.1016/0006-2952(61)90145-9 (1961).
14. Palop, J. J. & Mucke, L. Amyloid-β–induced neuronal dysfunction in Alzheimer's disease: from synapses toward neural networks. *Nat. Neurosci.* **13** (7), 812–818. https://doi.org/10.1038/nn.2583 (2010).
15. Bhatt, S., Bhatt, P. & Bhatt, M. Molecular dynamics simulation: a powerful tool for drug design and discovery. *Drug Discov Today*. **25** (5), 943–954 (2020).

Figures



Figure 1

Three-dimensional crystal structure of human acetylcholinesterase (AChE; PDB ID: 1EEA) prepared for molecular docking. The active-site gorge and catalytic triad residues (Ser203, His447, Glu334) are highlighted.

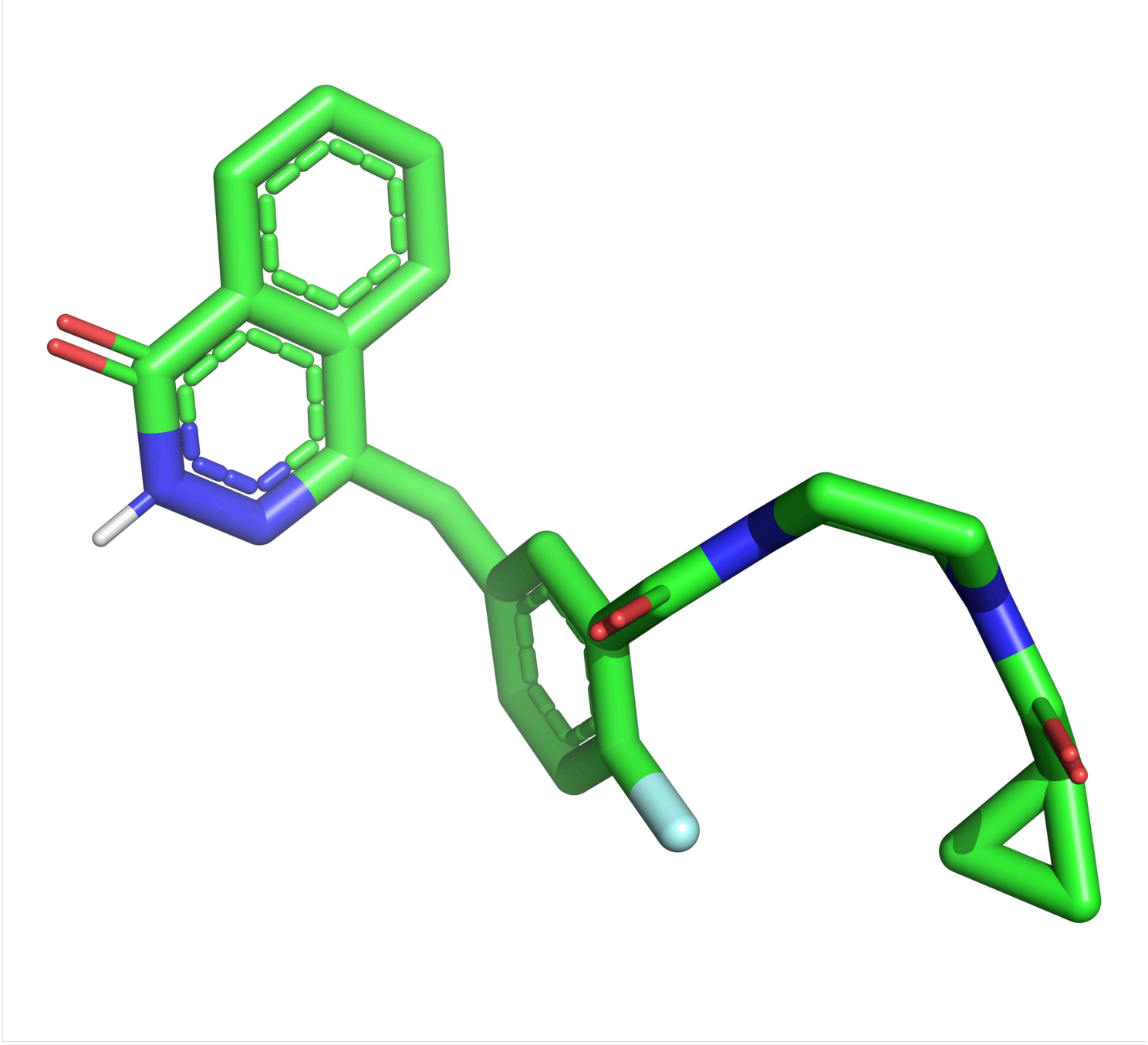


Figure 2

Two-dimensional chemical structure of olaparib (MW: 407.32 Da; MF: $C_{24}H_{23}FN_4O_3$), illustrating the phthalazinone core, fluorobenzyl moiety, and cyclopropyl-piperazine pharmacophore.

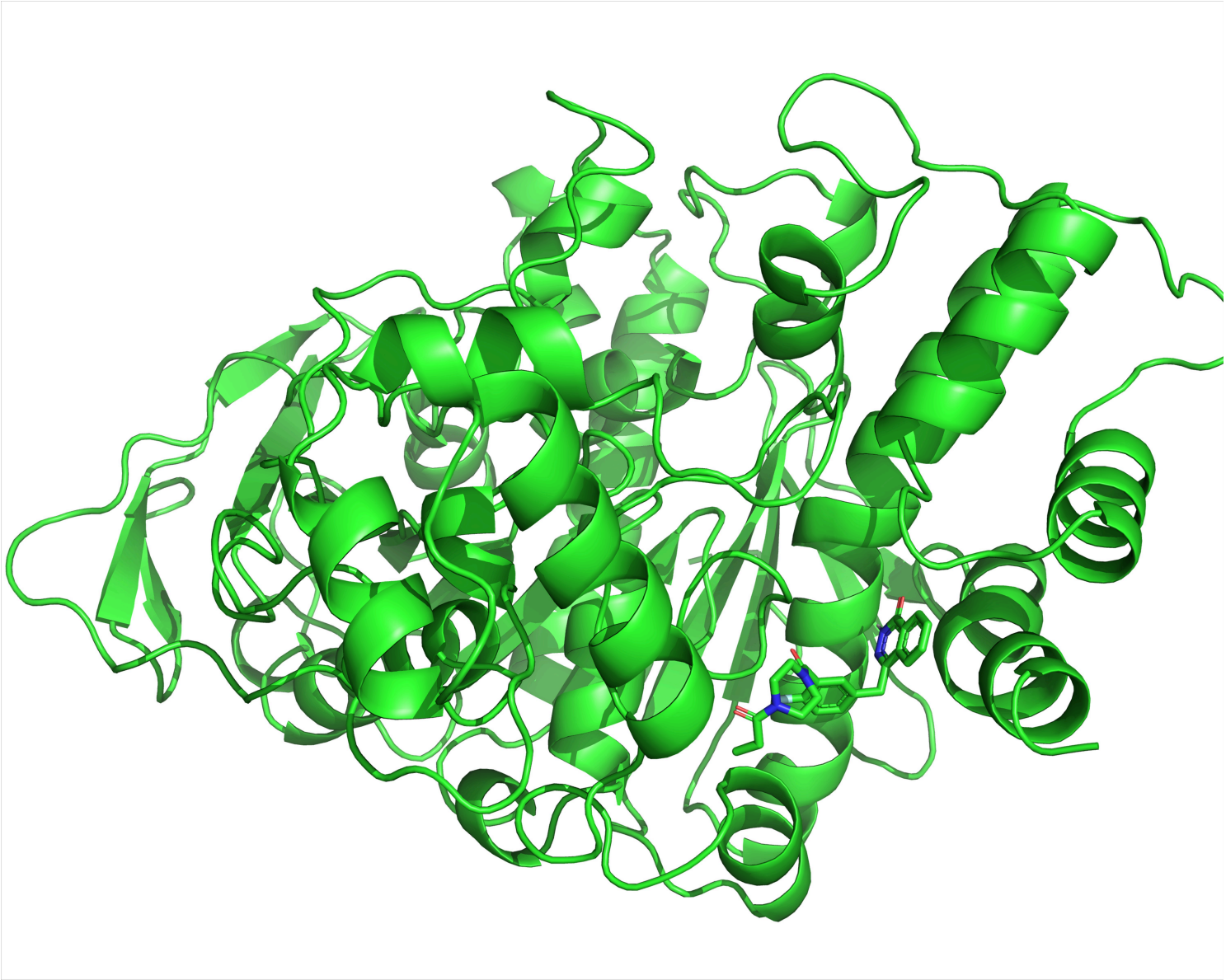


Figure 3

Molecular docking pose of olaparib within the AChE active-site gorge (PDB ID: 1EEA). Hydrogen bonds (yellow dashes) and hydrophobic contacts are indicated. Key interacting residues (Ser203, Tyr337, Trp86, Phe338) are labelled.

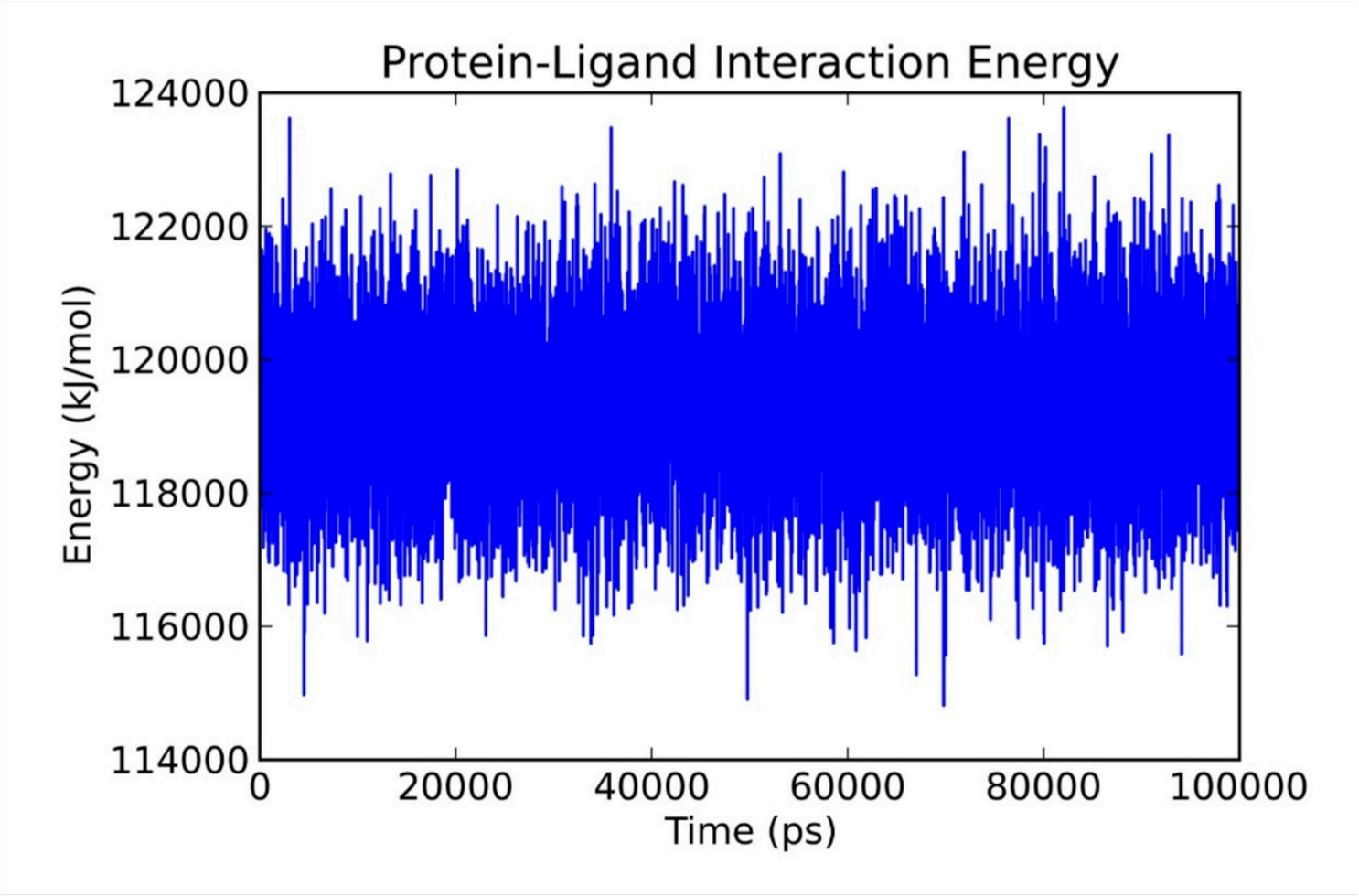


Figure 4

Total potential energy of the olaparib–AChE simulation system over 100 ns. Stable energy values following equilibration confirm thermodynamic convergence of the system.

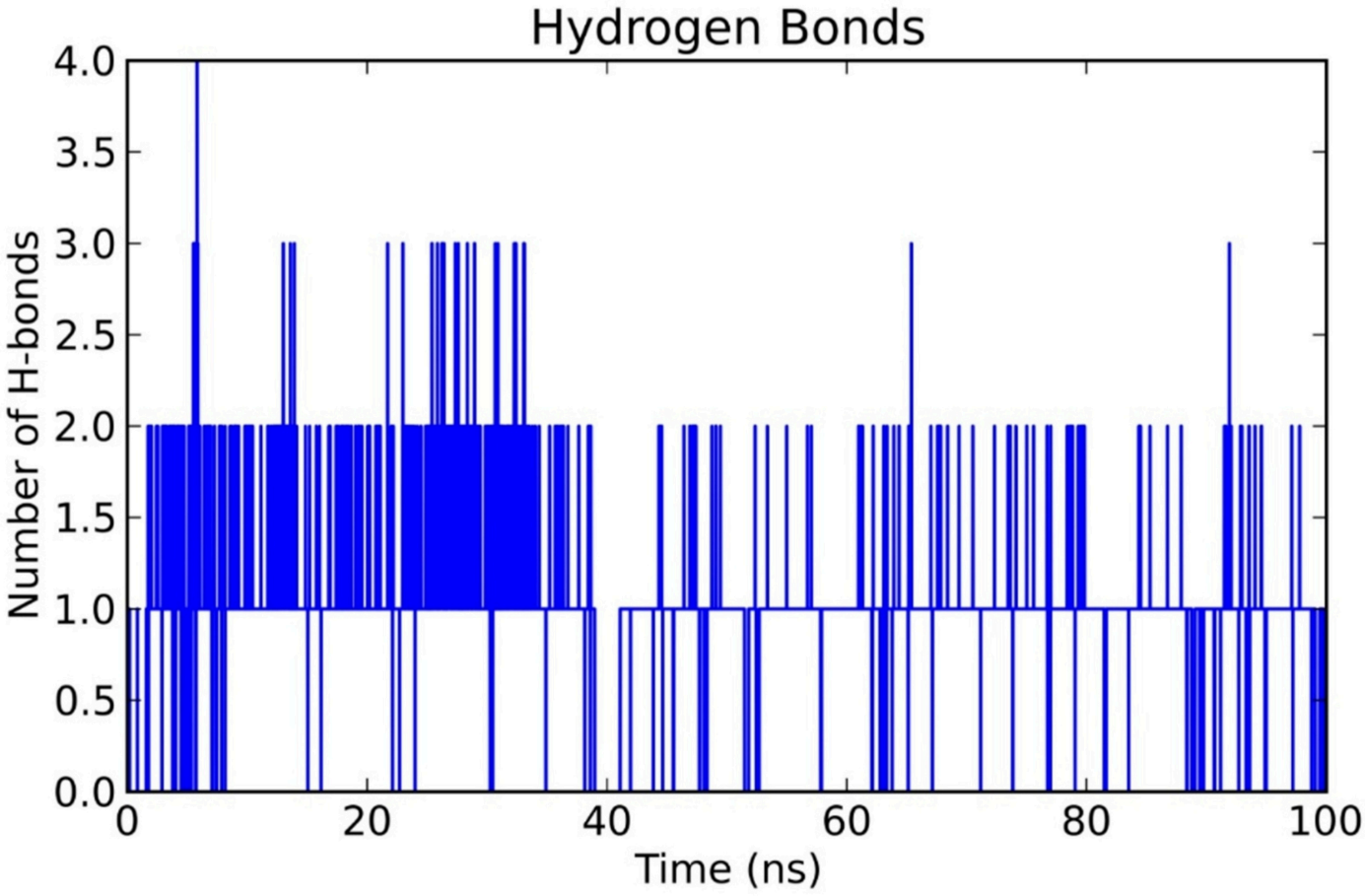


Figure 5

Number of hydrogen bonds between olaparib and AChE as a function of simulation time (100 ns). Persistent H-bond occupancy indicates stable polar interactions within the active-site gorge.

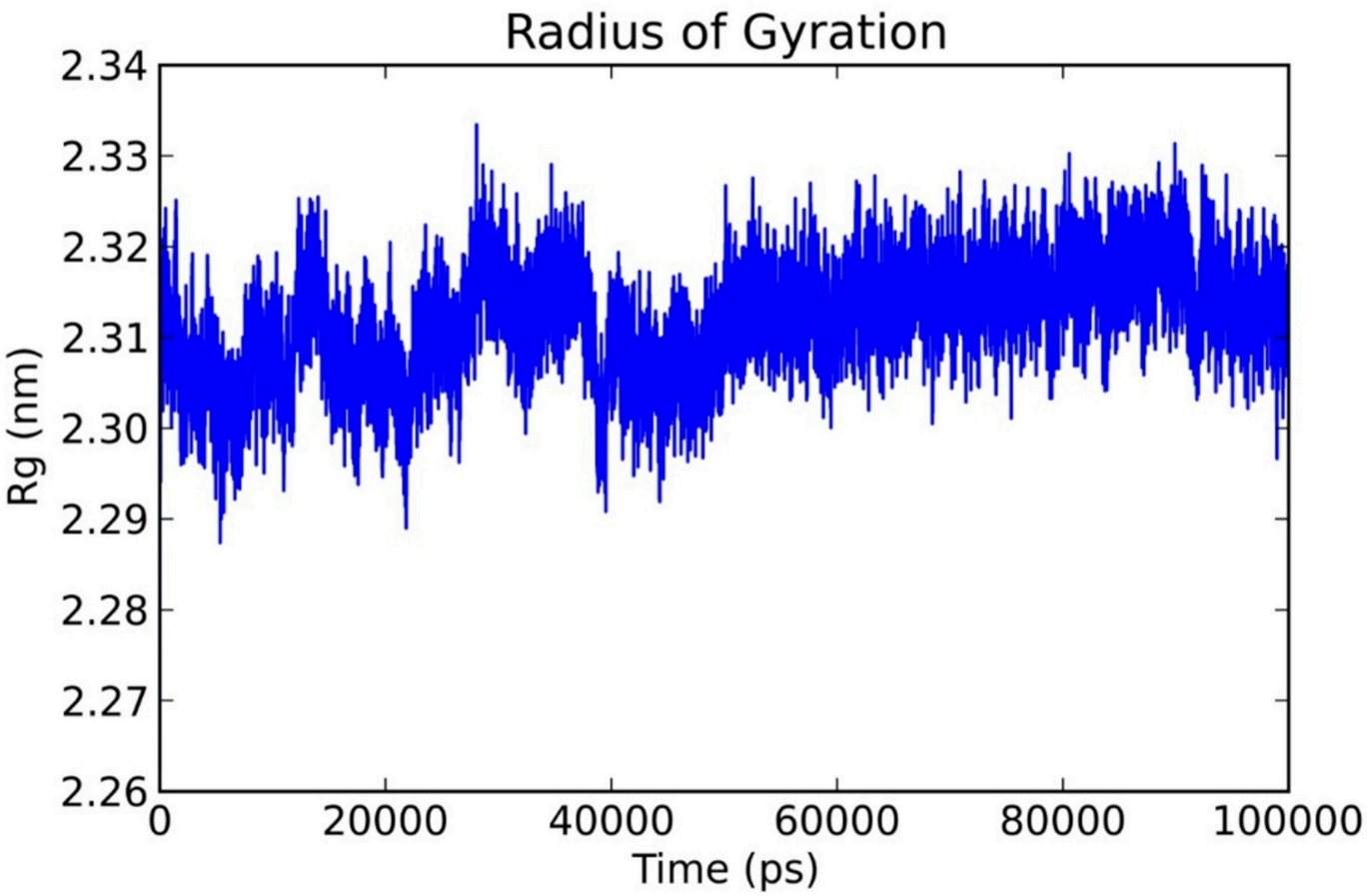


Figure 6

Radius of gyration (Rg) of the AChE–olaparib complex over 100 ns of MD simulation. Consistent Rg values confirm maintenance of protein compactness and structural integrity.

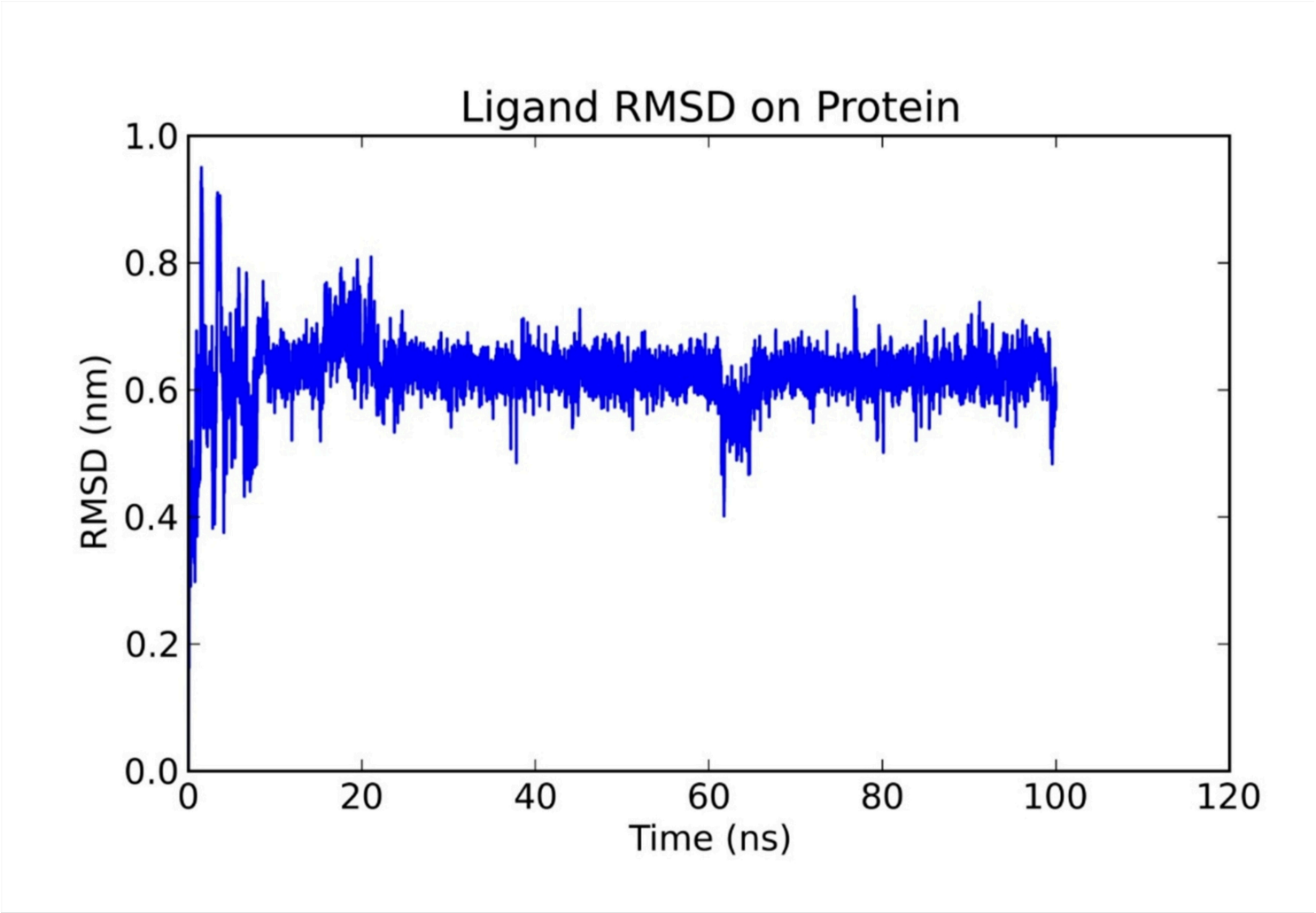


Figure 7

Ligand RMSD of olaparib relative to its initial docked position over 100 ns of MD simulation. Low and stable RMSD values confirm persistent binding within the AChE active-site gorge.

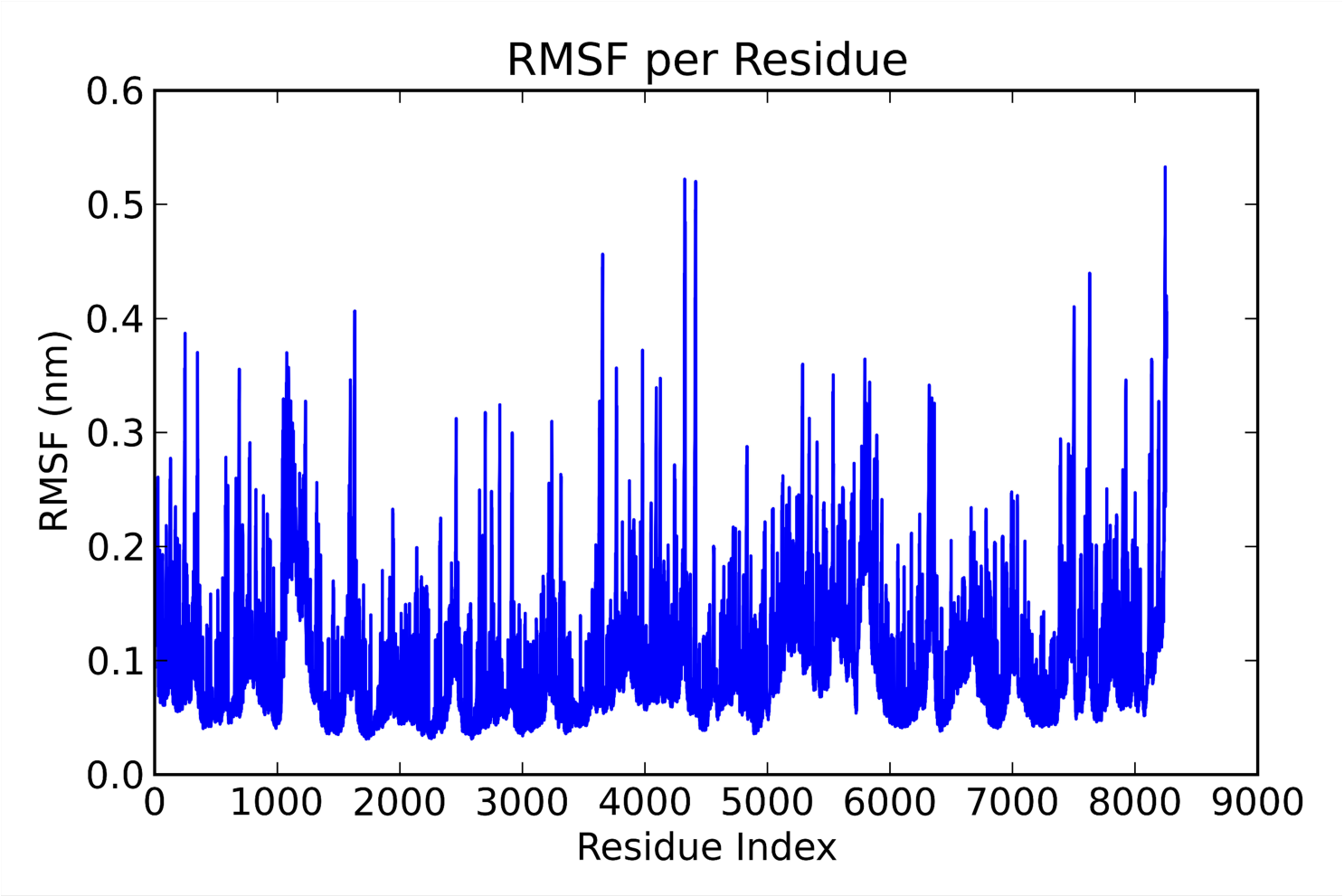


Figure 8

Per-residue RMSF of AChE during the 100-ns MD simulation in complex with olaparib. Low RMSF values for active-site residues (Trp86, Tyr337, Phe338, Ser203) confirm stable binding interface geometry.

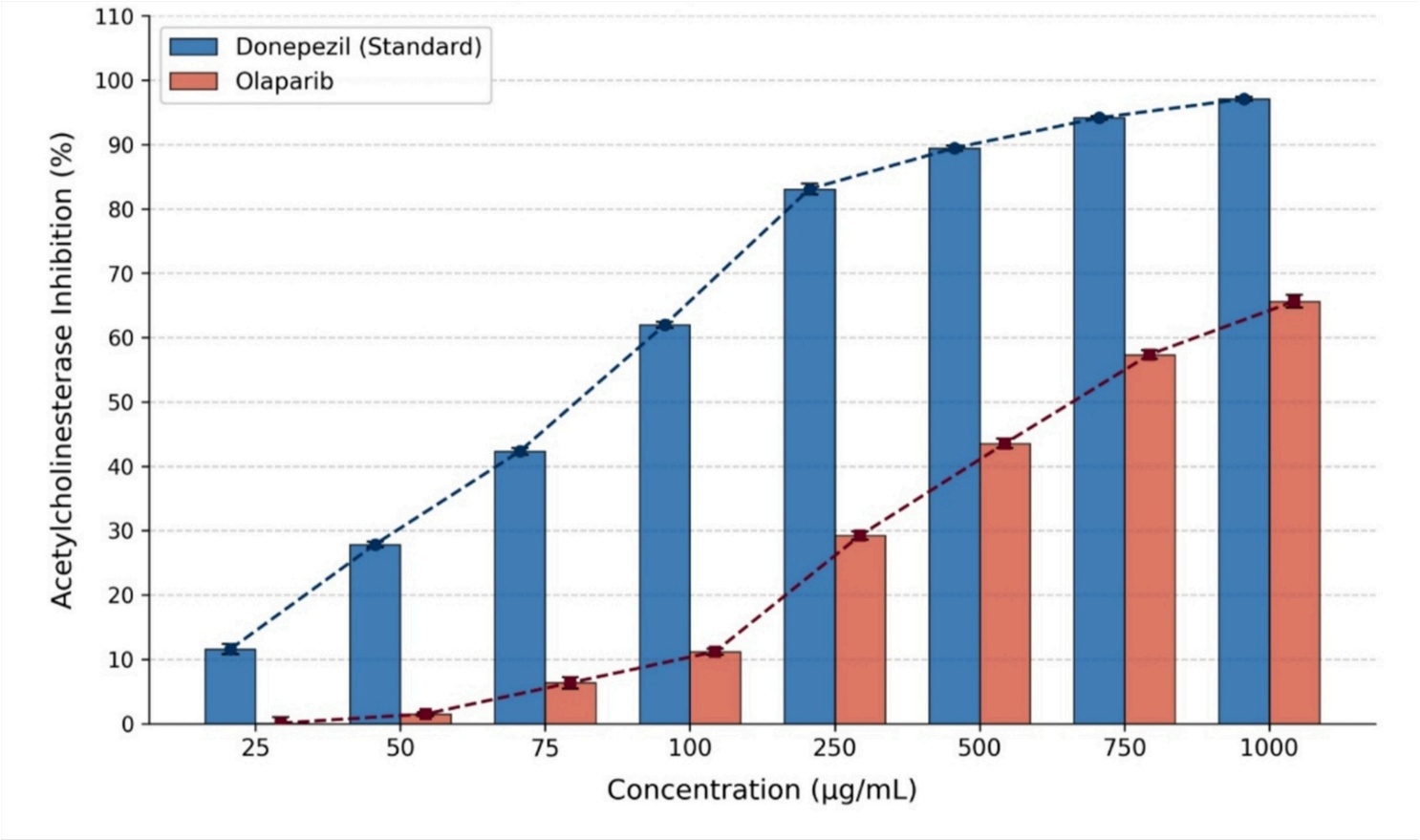


Figure 9

Comparative in vitro acetylcholinesterase inhibitory activity of olaparib and donepezil across concentrations of 25–1000 µg/mL. Bars represent mean % inhibition; error bars indicate SEM (n = 3). Donepezil demonstrates markedly higher inhibitory potency across all concentrations tested.

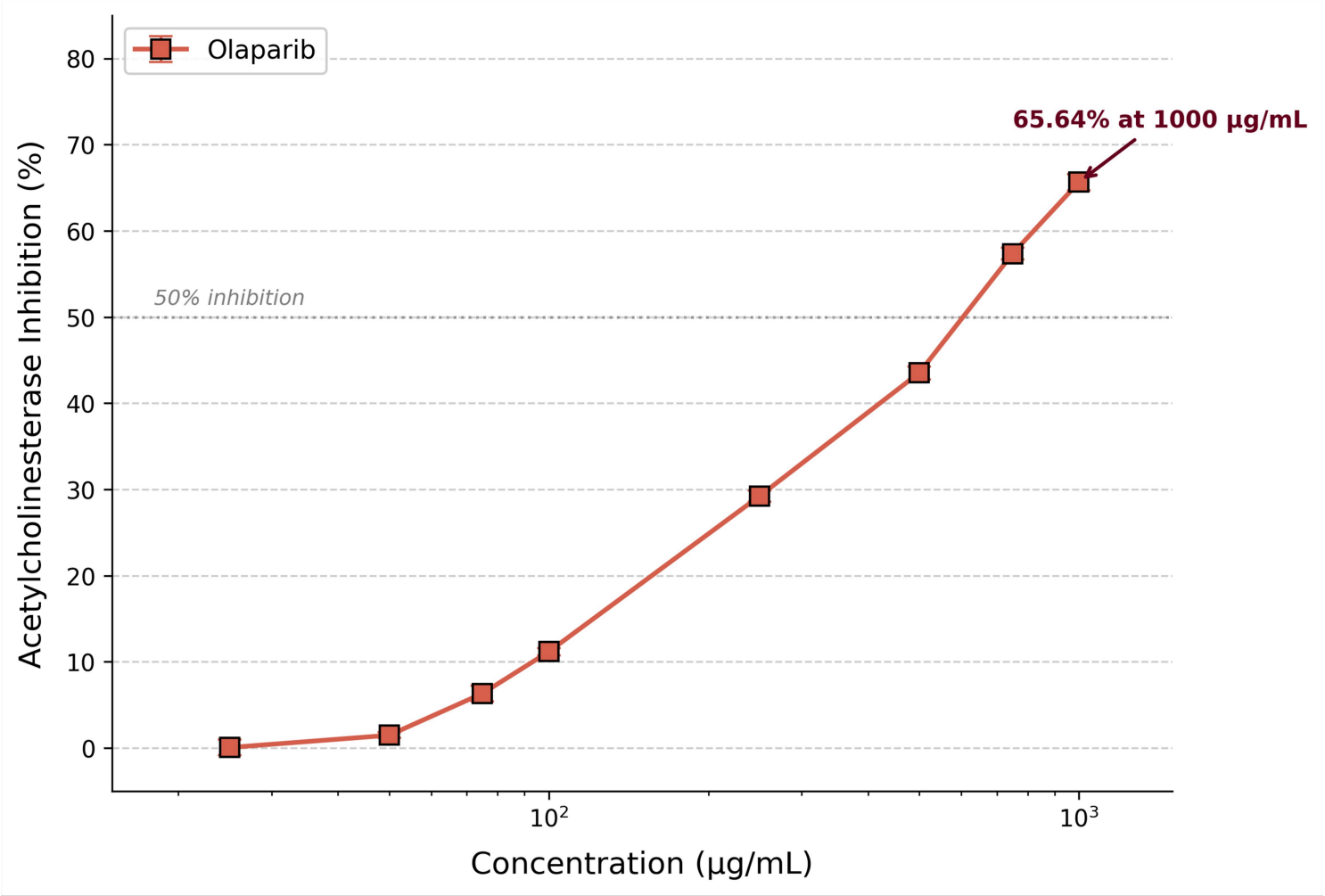


Figure 10

Dose–response curve of olaparib for in vitro acetylcholinesterase inhibition plotted on a logarithmic concentration axis. The dashed reference line indicates 50% inhibition. Maximum inhibition of 65.64 ± 0.96% was achieved at 1000 µg/mL; IC_{50} could not be determined within the tested concentration range.